*Human Molecular Genetics, 2003, Vol. 12, No. 18* **2321–2332**
*DOI: 10.1093/hmg/ddg243*

# A haplotype-based molecular analysis of CFTR mutations associated with respiratory and pancreatic diseases

**Ji Hyun Lee[1], Ji Ha Choi[1], Wan Namkung[1], John W. Hanrahan[5], Joon Chang[2], Si Young Song[2], Seung Woo Park[2], Dong Soo Kim[3], Joo-Heon Yoon[4], Yousin Suh[6], In-Jin Jang[7], Joo Hyun Nam[8], Sung Joon Kim[8], Mi-Ook Cho[9], Jong-Eun Lee[10], Kyung Hwan Kim[1] and Min Goo Lee[1,*]**

[1]Department of Pharmacology and Brain Korea 21 Project for Medical Science, [2]Department of Internal Medicine, [3]Department of Pediatrics and [4]Department of Otorhinolaryngology, Yonsei University College of Medicine, Seoul 120-752, Korea, [5]Department of Physiology, McGill University, Montreal, Quebec Canada, H3G 1Y6, [6]Department of Biochemistry and Molecular Biology and [7]Department of Pharmacology, Seoul National University College of Medicine, Seoul 110-799, Korea, [8]Department of Physiology, Sungkyunkwan University School of Medicine, Suwon 440-746, Korea, [9]Metagentech Co., 207-10 Poi-Dong, Kangnam-Gu, Seoul 135-963, Korea and [10]DNA Link Inc., 15-1 Yonhee-Dong, Seodaemun-Gu, Seoul 120-110, Korea

Received April 21, 2003; Revised June 20, 2003; Accepted July 7, 2003

**Aberrant membrane transport caused by mutations in the cystic fibrosis transmembrane conductance regulator (CFTR) gene is associated with a wide spectrum of respiratory and digestive diseases as well as cystic fibrosis. Using a gene scanning method, we found 11 polymorphisms and mutations of the *CFTR* gene in the Korean population. Individual variants at these sites were analyzed by conventional DNA screening in 117 control and 75 patients having bronchiectasis or chronic pancreatitis. In a haplotype determination based on a Bayesian algorithm, 15 haplotypes were assembled in the 192 individuals tested. Several haplotypes, especially with Q1352H, IVS8 $T_5$, and E217G, were found to have disease associations in a case–control study. Notably, a common polymorphism of M470V appears to affect the intensity of the disease association. Among the two haplotypes having IVS8 $T_5$, the $T_5$-V470 haplotype showed higher disease association than the $T_5$-M470 haplotype. In addition, a Q1352H mutation found in a V470 background showed the strongest disease association. The physiological significances of the identified mutations were rigorously analyzed. Non-synonymous E217G and Q1352H mutations in the M470 background caused a 60–80% reduction in CFTR-dependent $Cl^-$ currents and $HCO_3^-$-transport activities. Surprisingly, the additional M470V polymorphic variant with the Q1352H mutation completely abolished CFTR-dependent anion transport activities. These findings provide the first evidence on the importance of CFTR mutations in the Asian population. Importantly, the results also reveal that interactions between multiple genetic variants in *cis* affect the final function of the gene products.**

## INTRODUCTION

Loss of anion transport caused by mutations in the cystic fibrosis transmembrane conductance regulator (CFTR; MIM 602421) gene is associated with a wide spectrum of respiratory and pancreatic disorders, as well as classically defined cystic fibrosis (CF) (1–5). Currently, more than 1000 mutations of CFTR are registered with the Cystic Fibrosis Gene Analysis Consortium (CFGAC; www.genet.sickkids.on.ca/). Several mutations of CFTR, such as F508del, G542X and N1303K, are associated with severe CF phenotypes and display high disease penetrance. However, many other mutations are instead

*To whom correspondence should be addressed at: Department of Pharmacology, Yonsei University College of Medicine, 134 Sinchon-Dong, Seoul 120-752, Korea. Tel: +82 2 361 5221; Fax: +82 2 313 1894; Email: mlee@yumc.yonsei.ac.kr

 © *Oxford University Press 2003; all rights reserved*

Downloaded from https://academic.oup.com/hmg/article-abstract/12/18/2321/2355638 by guest on 13 October 2019

associated with monosymptomatic diseases of lung, pancreas or vas deferens, and show partial penetrance. Factors such as environmental effects can be employed to explain the heterogeneity of the disease phenotypes caused by mild mutations (6). An important approach for resolving these heterogeneous phenotypes is to characterize the haplotype background of each individual, especially for the intragenic regions of CFTR. Various interactions or additive effects between multiple mutations and/or polymorphic sites will code for the final destined function of the gene products. In addition, haplotype information is also useful for tracing the disease-associated gene flow in population history (7–9).

It is expected that, if any functional CFTR gene variations exist in the population, they are associated with epithelial disorders, since CFTR performs a critical role in the overall regulation of epithelial ion transport and there are no functional analogues or substitutes for this protein (10–14). Although mutations and polymorphisms of CFTR have been extensively studied in Western populations, its importance is less emphasized in East Asia due to the rare presentation of classical CF. However, other diseases reported to be associated with CFTR mutations, such as bronchiectasis and chronic pancreatitis, are also present in the East Asian population. Isolated pulmonary bronchiectasis has been regarded as a different clinical entity from CF, though bronchiectasis is a common feature of CF. However, it was suggested that certain cases of monosymptomatic bronchiectasis are also associated with CFTR mutations (2). Similarly, a couple of recent reports showed that significant proportions of monosymptomatic chronic pancreatitis patients had CFTR mutations (3,4). Therefore, we investigated the possibility of an association between genetic variations of CFTR and these diseases in the Korean population by using integrated gene analysis in combination with molecular and functional studies.

Gene scanning and haplotype assembly revealed that the background haplotype for F508del (8), which accounts for 66% of worldwide cystic fibrosis, is very rare in the Korean population. However, several other haplotypes, especially mutations with decreased membrane expression and reduced $HCO_3^-$ transport, were found to be associated with respiratory or pancreatic diseases. Notably, an additional polymorphic variation of M470V affects the intensity of disease association and the anion transport function of CFTR protein. The present study is the first comprehensive report demonstrating the significance of CFTR variants in association with chronic respiratory and pancreatic diseases in East Asians. Moreover, the results also reveal that interaction between multiple genetic variants in *cis* affect the function of CFTR gene products.

## RESULTS

### Genetic variants of CFTR in the Korean population

The genetic variants of CFTR have not been thoroughly investigated in East Asians due to the rare incidence of classical CF. Therefore, initially we undertook to find the common CFTR mutations and polymorphisms in the Korean population. We used the two-dimensional gene scanning (TDGS) technique to efficiently scan entire CFTR exons. Although a TDGS trial for the exploration of human CFTR has been described previously (15), a whole set of primers were newly designed for the optimal PCR amplification, denaturing gradient gel electrophoresis (DGGE) separation, and DNA-fragment distribution in two-dimensional gel (Supplement). The resulting test permitted the detection of mutations and polymorphisms in CFTR coding regions as well as splice site mutations.

TDGS was performed on a total of 100 samples from 28 healthy controls, 47 bronchiectasis patients, and 25 chronic pancreatitis patients. Typical TDGS patterns are shown in Figure 1. In samples from healthy control subjects, two heteroduplex bands were frequently seen in exons 10 and 14a, and identified as M470V and 2694T/G (T854), respectively. In samples from patients, several other heteroduplexes were found including one in exon 22, which was identified as Q1352H (G to C change at nucleotide 4188). After comprehensive gene scanning and subsequent nucleotide sequencing, we found nine diallelic variations in 5′-UTR and in several exons (Table 1, left column). Among them, two were novel mutations and the other seven had been previously registered in CFGAC.

### Genotype frequencies in control and patient groups

To investigate the pathological association between CFTR genetic variations and bronchiectasis or chronic pancreatitis, a case–control study was performed using samples from 192 subjects as detailed in Materials and Methods. In addition to the nine variations found by TDGS, we included the 10 most common worldwide disease-causing mutations (data obtained from CFGAC) and a possible disease-associated microsatellite, IVS8 $T_n$ (Table 1). Diallelic loci were analyzed by an automated DNA screening (SNaPshot; Applied Biosystems Inc.), and the $T_n$ numbers were identified by bi-directional nucleotide sequencing. Among the 10 worldwide disease-causing mutations, only one case of R117H was found in a control subject. The genotype frequencies found at each locus are listed in Table 2.

Genetic variants at several sites were found to be associated with bronchiectasis and/or chronic pancreatitis, the most notable being Q1352H. The heterozygote frequency of Q1352H was significantly higher in bronchiectasis ($P = 0.02$) and chronic pancreatitis patients ($P = 0.005$) than in the control group. The frequency of E217G also seemed to be higher in bronchiectasis patients, especially in the subgroup of child bronchiectasis ($P = 0.04$; ages under 18, three cases in 20 patients), although it was not significant when all patients were included ($P = 0.10$; four cases in 47 patients). It has been suggested that IVS8 $T_5$ is associated with CF or monosymptomatic CF-related diseases by affecting RNA splicing (16). The present data also showed the increased frequency of IVS8 $T_5$ in the patient groups, especially in those with bronchiectasis ($P = 0.03$). Since a total of 22 comparisons were made on 11 loci, their overall significances were evaluated using the information from all loci examined by two different approaches, the Bonferroni technique and the summation of chi-square statistics (17). When applying the conservative Bonferroni technique, no individual *P*-values in Table 2 were smaller than the Bonferroni significance (0.0023; $\alpha$/number of comparison = 0.05/22). However, the summed chi-square

Downloaded from https://academic.oup.com/hmg/article-abstract/12/18/2321/2355638 by guest on 13 October 2019

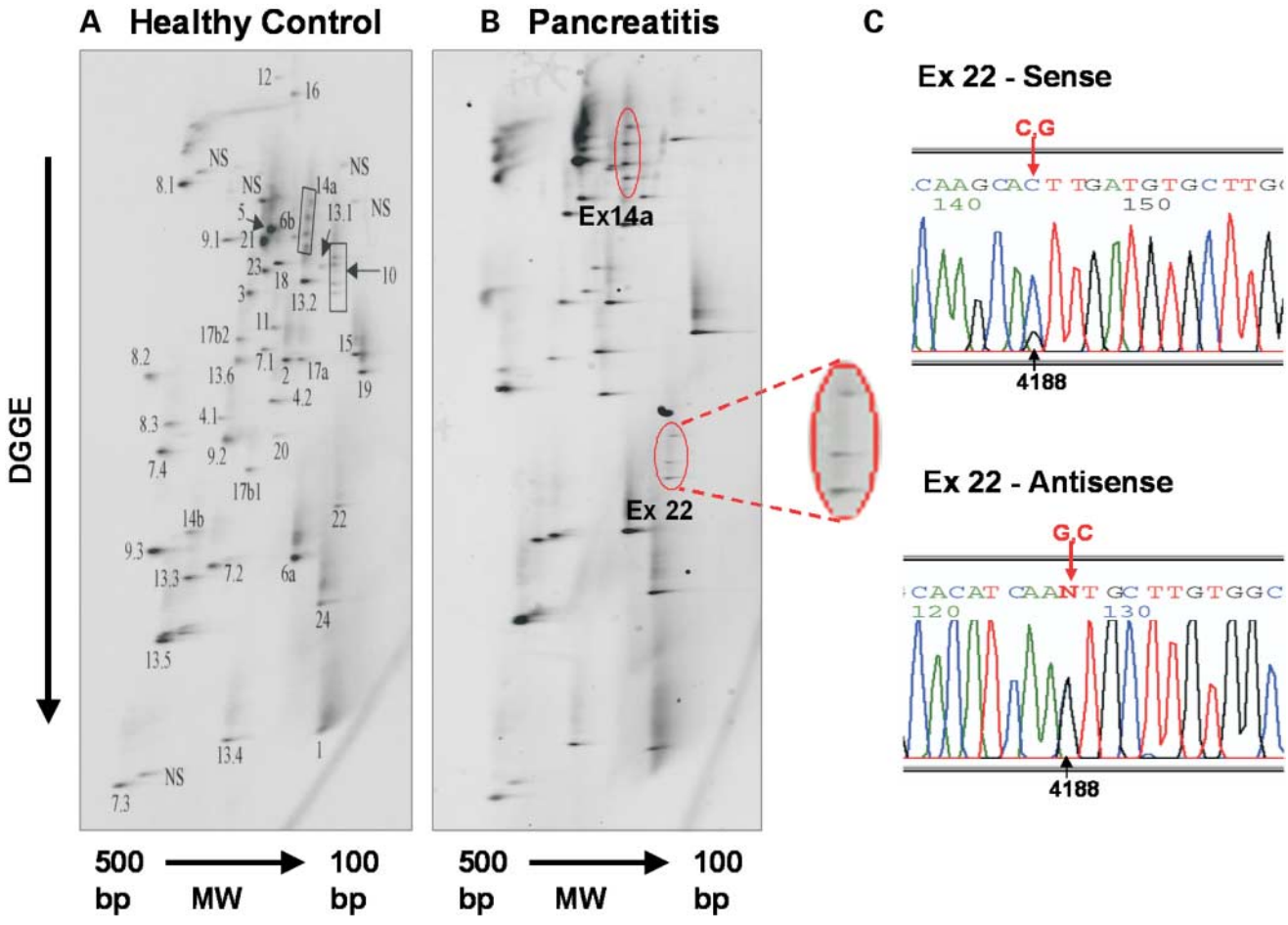


**Figure 1.** Two-dimensional gene scanning (TDGS) of human CFTR. The entire CFTR coding regions and parts of the introns were amplified by two-step PCR, as described in Materials and Methods. Forty-one short PCR fragments were distributed in two-dimensional gels according to their molecular weights and melting temperatures (DGGE). (**A**) A sample from a control subject shows heteroduplex bands in exons 10 and 14a. (**B**) A sample from a pancreatitis patient shows heteroduplex bands in exons 14a and 22. (**C**) The genetic variation in exon 22 was identified as Q1352H (4188G > C) by bi-directional nucleotide sequencing.

**Table 1.** CFTR genetic variants analyzed in this study

| Variations found by TDGS | Most common worldwide disease-causing mutations | Reported disease-associated microsatellite |
|---|---|---|
| −8G/C (5′UTR)[a] | R117H (exon 4) | $T_{5\text{-}7,9}$ (IVS 8) (16) |
| I125T (exon 4)[b] | 621 + 1G > T (intron 4) | |
| E217G (exon 6a)[b] | F508del (exon 10) | |
| 1059C > T (exon 7, A309)[a] | 1717-1G > A (intron 10) | |
| M470V (exon 10)[b] | G542X (exon 11) | |
| I556V (exon 11)[b] | G551D (exon 11) | |
| 2694T/G (exon 14a, T854)[b] | R553X (exon 11) | |
| Q1352H (exon 22)[b] | R1162X (exon 19) | |
| R1453W (exon 24)[b] | W1282X (exon 20) | |
| | N1303K (exon 21) | |

Mutation names and nucleotide numbers are presented according to the Cystic Fibrosis Genetic Analysis Consortium (CFGAC; www.genet.sickkids.on.ca/).
[a]New genetic variations found in this study.
[b]Registered variations in CFGAC.

strongly suggested differences among individual groups ($P = 0.00015$; $\chi^2 = 54.1$, degree of freedom = 22). Therefore, the present data set is a typical example that the two different approaches for multiple comparisons do not agree (17).

### Haplotype patterns and their disease associations

Since multiple alleles exist in both controls and patients, a haplotype-based approach was used to provide a better understanding of the disease-associated CFTR variations. Haplotypes were assembled using the genotype data obtained from the 192 tested samples and the Haplotyper program based on the Bayesian algorithm (7). Eleven loci consisting of 10 diallelic variants and a microsatellite of IVS8 $T_n$ were analyzed. Since the program accepts only diallelic data, in the case of IVS8 $T_n$, $T_5$ was considered as mutant and all other alleles were inputted as wild-type (WT). Although a true haplotype can be resolved by experimental molecular methods, it is not practical for large-scale haplotype determinations. Since it has been shown that the average error rate of the Bayesian method is less than 0.01 for samples of 100 individuals with 20 loci

Downloaded from https://academic.oup.com/hmg/article-abstract/12/18/2321/2355638 by guest on 13 October 2019

**Table 2.** Frequency of CFTR gene variants in the Korean population

| Variation | Genotype | Group (number) | | |
|---|---|---|---|---|
| | | Healthy control ($n=117$) | Bronchiectasis ($n=47$) | Pancreatitis ($n=28$) |
| *Diallelic* | | | | |
| -8G/C | +/+ | 105 | 44 | 22 |
| | +/−[a] | 12 | 3 | 6 |
| R117H | +/+ | 116 | 47 | 28 |
| | +/− | 1 | 0 | 0 |
| I125T | +/+ | 116 | 46 | 27 |
| | +/− | 1 | 1 | 1 |
| E217G | +/+ | 114 | 43 | 27 |
| | +/− | 3 | **4**[b] | 1 |
| 1059C > T | +/+ | 117 | 47 | 27 |
| (A309) | +/− | 0 | 0 | 1 |
| M470V | +/+ | 23 | 3 | 6 |
| | +/− | 52 | 28 | 14 |
| | −/− | 42 | 16 | 8 |
| I556V | +/+ | 111 | 45 | 28 |
| | +/− | 6 | 2 | 0 |
| 2694T/G | +/+ | 41 | 16 | 8 |
| (T854) | +/− | 51 | 27 | 14 |
| | −/− | 25 | 4 | 6 |
| Q1352H | +/+ | 116 | 43 | 24 |
| | +/− | 1 | **4*** | **4**** |
| R1453W | +/+ | 115 | 46 | 28 |
| | +/− | 2 | 1 | 0 |
| *Microsatellite* | | | | |
| $T_{5\text{-}7,9}$ | 5/7 | 4 | **6*** | 2 |
| (IVS 8) | 6/7 | 0 | 1 | 0 |
| | 7/7 | 110 | 39*[c] | 26 |
| | 7/9 | 3 | 1 | 0 |

Differences between control and disease groups were analyzed by a chi-square test. When an expected cell value was less than 5, Fisher's exact test was used. Significant increases in the disease cases are presented in bold.
[a]Minus signs (−) indicate the variant type of diallelic variations.
[b]$P=0.04$, in the case of child bronchiectasis (ages under 18, 3 cases in 20 patients).
[c]Decreased frequency in the disease cases. *$P<0.05$, **$P<0.01$ difference from control.

(partition–ligation algorithm in 7) and we used a larger population (192 individuals) with fewer gene variations (11 sites), the error rate is expected to be far less than 0.01 in the present haplotype determination.

After 100 rounds of iterations, 15 haplotypes were assembled and their identification (ID) numbers were assigned according to the total sample frequencies (Table 3). In the initial step, we classified each haplotype using two common polymorphisms of M470V and 2694T/G (Table 3, right-most column). One interesting observation was of a tight association between the M470V and the 2694T/G (T854) loci. With the exception of haplotypes 8 (2–2), 12 (1–1), and 13 (2–2), all other haplotypes, that is 97% of the control population, were in the background of either V470-2694T (2–1) or M470-2694G (1–2). Therefore, haplotypes 4, 5, 7, 11 and 14 seem to be the variants of haplotype 1, and haplotypes 3, 6, 9, 10 and 15 be the variants of haplotype 2. It was found that haplotype 12 has IVS8 $T_9$ by a different set of haplotype assembly using $T_9$ as mutant instead of $T_5$. Therefore, haplotype 12 was found to have IVS8 $T_9$-M470-2694T, and it has been reported that 95% of F508del mutants arise from this haplotype (8). Notably, the allele frequency of haplotype 12 in the control Korean population (0.9%) was much less than that in the Caucasian population (7.3%).

Although the frequency of haplotype 1, which has V470, was highest in the Korean population, we used haplotype 2, which has M470, as a standard haplotype for statistical analysis since the sequence of haplotype 2 matches with the registered CFTR sequences in most databases. In addition, it was reported that V470 CFTR has about a half of the M470 CFTR function, when whole cell $Cl^-$ channel activities were compared (16). Haplotypes showing extremely low frequencies (<2%) in all groups (haplotypes 8–15) were excluded from the statistical analysis. Similar to the genotype data (Table 2), none of the comparisons in haplotype data (Table 3) reached the Bonferroni significance (0.004; $\alpha$/number of comparison = 0.05/12). However, the overall chi-square value again suggested a frequency difference between the control and the patient groups ($P=0.014$; $\chi^2=26.2$, degree of freedom = 12).

As expected from the genotype data, haplotype 4 containing Q1352H showed the strongest association with bronchiectasis and chronic pancreatitis in the Korean population ($P=0.02$ and $P=0.008$, respectively). The frequency of haplotype 6 containing E217G was 5.8-fold higher in child bronchiectasis patients (7.5%, three in 40; $P=0.03$) than that in the control population (1.3%, three in 234), although this was not significant for all bronchiectasis patients (4.3%, four in 94; $P=0.08$). The genotype data showed a possible association between IVS8 $T_5$ and bronchiectasis (Table 2). In the haplotype assembly of Table 3, haplotypes 5 and 9 were found to have IVS8 $T_5$. The frequencies of haplotypes 5 and 9 were similar in control populations. Interestingly, the frequency of haplotype 5 containing another variation of V470 was significantly increased in bronchiectasis group ($P=0.02$), while that of haplotype 9 containing M470 was not changed.

### Molecular and functional studies on single mutants

A molecular and functional study of the CFTR mutations was performed to draw concrete conclusions on the disease associations and to identify the underlying mechanisms of defective CFTR function. Among the non-synonymous mutations identified in the Korean population, four were selected for functional study based on the results from the present study and from information reported to the CFGAC (Table 4). To isolate each mutation-induced effect, all mutations were introduced into the same haplotype 2 background, which contains M470.

Many disease-causing CFTR mutations produce folding or maturation defects (18,19). Therefore, we initially studied the protein expression levels of each mutant. WT and mutant pNUT-CFTR clones were transfected to CHO-K1 cells and stable transfectants were selected using methotrexate. After lysing the cells, proteins were harvested and blotted with antibodies against CFTR. Similar to that found by previous reports, complex-glycosylated 'band C' proteins were principally detected in the CHO cell systems rather than the primary-translated 'band A' or the core-glycosylated 'band B' forms (16). As shown in Figure 2A, the protein expressions of mature glycosylated CFTR were significantly decreased in E217G and Q1352H mutations. Similar expression levels of dihydrofolate reductase (DHFR), a *cis*-gene product in the expression vector, in each transfectant

Downloaded from https://academic.oup.com/hmg/article-abstract/12/18/2321/2355638 by guest on 13 October 2019

**Table 3.** Haplotype assembly

| Allele ID | -8G/C | R117H | I125T | E217G | 1059C/T | $T_{5\text{-}7,9}$ | M470V | I556V | 2694T/G | Q1352H | R1453W | Group | | | [a]M470V-2694T/G background |
|---|---|---|---|---|---|---|---|---|---|---|---|---|---|---|---|
| | | | | | | | | | | | | Control, *n* (%) | Bronchiectasis, *n* (%) | Pancreatitis, *n* (%) | |
| 1 | G | R | I | E | C | WT[b] | **V** | I | T | Q | R | 121 (51.7) | 47 (50.0) | 24 (42.9) | 2–1 |
| 2 | G | R | I | E | C | WT | M | I | **G** | Q | R | 78 (33.3) | 25 (26.6) | 18 (32.1) | 1–2 |
| 3 | **C** | R | I | E | C | WT | M | I | G | Q | R | 11 (4.7) | 3 (3.2) | 5 (8.9) | 1–2 |
| 4 | G | R | I | E | C | WT | **V** | I | T | **H** | R | 1 (0.4) | 4 (4.3)* | 4 (7.1)** | 2–1 |
| 5 | G | R | I | E | C | **5** | V | I | T | Q | R | 2 (0.9) | 5 (5.4)* | 1 (1.8) | 2–1 |
| 6 | G | R | I | **G** | C | WT | M | I | **G** | Q | R | 3 (1.3) | 4 (4.3)[c] | 1 (1.8) | 1–2 |
| 7 | G | R | I | E | C | WT | **V** | **V** | T | Q | R | 5 (2.1) | 2 (2.2) | 0 (0.0) | 2–1 |
| 8 | G | R | I | E | C | WT | V | I | **G** | Q | R | 4 (1.7) | 1 (1.0) | 0 (0.0) | 2–2 |
| 9 | G | R | I | E | C | **5** | M | I | G | Q | R | 2 (0.9) | 1 (1.0) | 1 (1.8) | 1–2 |
| 10 | G | R | I | E | C | WT | M | I | G | Q | **W** | 2 (0.9) | 1 (1.0) | 0 (0.0) | 1–2 |
| 11 | G | R | **T** | E | C | WT | **V** | I | T | Q | R | 1 (0.4) | 1 (1.0) | 1 (1.8) | 2–1 |
| 12 | G | R | I | E | C | WT | M | I | T | Q | R | 2 (0.9) | 0 (0.0) | 0 (0.0) | 1–1 |
| 13 | **C** | R | I | E | C | WT | **V** | I | **G** | Q | R | 1 (0.4) | 0 (0.0) | 0 (0.0) | 2–2 |
| 14 | G | **H** | I | E | C | WT | V | **V** | T | Q | R | 1 (0.4) | 0 (0.0) | 0 (0.0) | 2–1 |
| 15 | **C** | R | I | E | **T** | WT | M | I | **G** | Q | R | 0 (0.0) | 0 (0.0) | 1 (1.8) | 1–2 |
| | | | | | | | | | | | Total | 234 (100.0) | 94 (100.0) | 56 (100.0) | |

Haplotypes were assembled using a software based on the Bayesian algorithm (Haplotyper) (7). Allele identification numbers were assigned according to the total frequency of haploid genes analyzed in this study. Differences between control and disease groups were analyzed by the chi-square test or Fisher's exact test (expected cell value <5) using the frequency of haplotype 2 as standard.

[a]M470V-2694T/G background was analyzed to classify each haplotype.

[b]$T_6$, $T_7$ and $T_9$ were regarded as wild-type.

[c]$P = 0.03$, in the case of child bronchiectasis (ages under 18, 10 cases of haplotype 2 and 3 cases of haplotype 6 in 40 haploid genes). *$P < 0.05$, **$P < 0.01$ difference from control.



Downloaded from https://academic.oup.com/hmg/article-abstract/12/18/2321/2355638 by guest on 13 October 2019

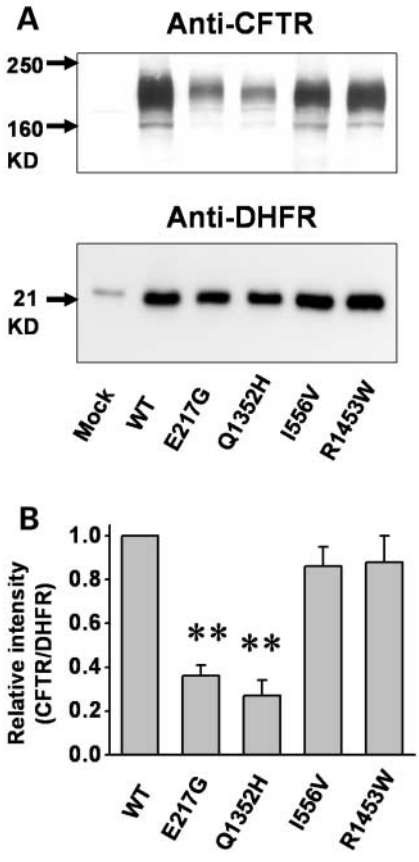


**Figure 2.** Protein expression in WT and mutant CFTR. (**A**) CHO-K1 cells stably expressing WT or mutant CFTR were lysed, proteins were harvested and blotted with monoclonal antibodies against NBD2 of CFTR and a *cis*-transfection marker DHFR. (**B**) Staining intensities of CFTR and DHFR bands were analyzed and the intensity ratios of CFTR/DHFR were compared. Results from four separate experiments were summarized.

verified that the results were not due to a lower transfection efficiency. Compared with WT, the expression levels of E217G and Q1352H were reduced by 64 and 73%, respectively, when CFTR band intensities were normalized against those of the *cis*-gene product DHFR (Fig. 2B).

CFTR protein has a $Cl^-$ channel function (20,21). Thus, the chloride channel activities of WT and mutant CFTR were measured in both whole-cell and single-channel configurations. In the whole cell current measurements, cAMP cocktail (5 μM forskolin plus 100 μM IBMX) treatment produced a large current in the NMDG-Cl solutions with linear I-V relationships (Fig. 3A and B). Treatment of glibenclamide (100 μM) or *N*-phenylanthranilic acid (DPC, 100 μM) inhibited this current by $76 \pm 4$ and $89 \pm 5\%$, respectively (not shown). These characteristics were in line with the previous observations on CFTR $Cl^-$ currents (11). Interestingly, all the mutants showed lower current densities (pA/pF) than WT CFTR. Among them, Q1352H showed the largest decrease (by 71%) and R1453W showed the smallest decrease (by 37%) in whole cell $Cl^-$ currents (Fig. 3C).

Single channel kinetics were analyzed in cell-attached configurations, since the protein expression levels (Fig. 2) did not perfectly match with the whole cell $Cl^-$ currents (Fig. 3C). No spontaneous channel activity was observed prior to the addition of cAMP cocktail. When the cells were stimulated with cAMP cocktail, low conductance currents were induced. Current records of 6 min duration at −80 mV (Fig. 3D) were analyzed for open probability (Po) and the results obtained were summarized as a bar graph (Fig. 3F). Compared with WT, Po was significantly reduced in I556V (by 34%), Q1352H (by 55%), and R1453W (by 78%). To determine the size of a single channel conductance, all point histograms were made at each voltage from −120 to +120 mV (in increments of 40 mV) and fitted to a Gaussian distribution. An example at +80 mV is shown in Figure 3E. The average conductance of WT CFTR was 7.6 pS and no significant changes were observed in the mutant CFTRs. Therefore, it was concluded that the decreased current density in the whole cell $Cl^-$ current of E217G (Fig. 3C) was due to the decreased membrane expression, and those of I556V and R1453W were due to the decreased Po. In the case of Q1352H, both membrane expression and Po were decreased.

Recently, it was found that CFTR plays an important role in transepithelial $HCO_3^-$ transport by regulating $Cl^-/HCO_3^-$ exchange (11–14). Reduced $HCO_3^-$ secretion by defective CFTR-dependent $HCO_3^-$ transport has been suggested to be an important pathologic mechanism in mutant CFTR-induced respiratory and pancreatic diseases (22,23). Therefore, $Cl^-/HCO_3^-$ exchange activities were measured in WT and mutant CFTR transfected cells by estimating $pH_i$ increase due to $Cl^-$ removal from the $HCO_3^-$-buffered perfusate (Fig. 4). In mock transfected cells, basal $Cl^-/HCO_3^-$ exchange activity was $0.083 \pm 0.05$ ΔpH unit/min and this was not significantly changed by forskolin treatment. However, in the WT-CFTR transfected cells, basal activity was increased to $0.141 \pm 0.021$ and forskolin treatment highly stimulated $Cl^-/HCO_3^-$ exchange to $0.677 \pm 0.063$ (Fig. 4A). To isolate CFTR-dependent $Cl^-/HCO_3^-$ exchange, cAMP-activated changes were calculated and analyzed in each mutant (Fig. 4B). Compared to the WT, E217G and Q1352H showed significant reductions in forskolin-stimulated $Cl^-/HCO_3^-$ exchange by 65 and 77%, respectively.

### Effects of M470V on Q1352H

The Q1352H mutation showed the highest disease associations in the genotype data. Since Q1352H is appeared only in the V470 background in the tested population (Table 3), we made M470V changes in WT- and Q1352H-CFTR clones and performed functional studies. As shown in Figure 5A, additional M470V change did not alter the protein expression levels in either WT- or Q1352H-CFTR. However, additional M470V change in Q1352H abolished cAMP-activated $Cl^-$ currents (Fig. 5C and D) and cAMP-activated $Cl^-/HCO_3^-$ exchanges (Fig. 5E and F) by 99 and 95%, respectively.

## DISCUSSION

The present study is the first comprehensive report on disease-associated CFTR gene variations in the East Asian population. CFTR mutation/polymorphism patterns in the Korean population were found to be quite different from those observed in the Caucasian populations. Among the 10 common worldwide disease-causing mutations, only one case of R117H was found

Downloaded from https://academic.oup.com/hmg/article-abstract/12/18/2321/2355638 by guest on 13 October 2019

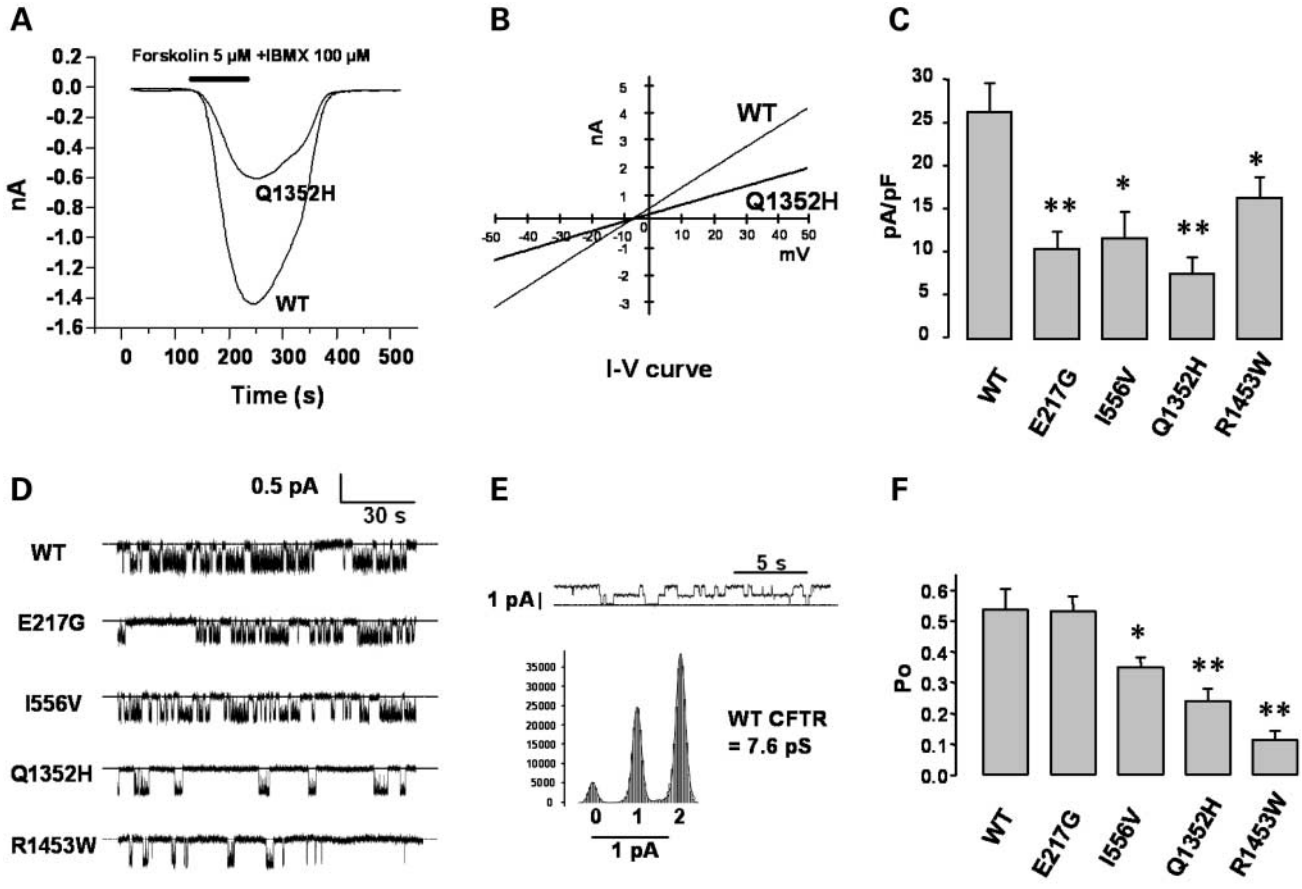


**Figure 3.** $Cl^-$ channel activities of WT and mutant CFTR. (**A–C**) $Cl^-$ currents were measured in the whole cell configuration. After establishing the whole cell configuration with NMDG-Cl rich solutions, CFTR was activated using a cAMP cocktail, 5 μM forskolin and 100 μM IBMX. Currents were recorded at a holding potential of −30 mV (A) and peak currents were normalized as current densities (pA/pF) (C). The *I–V* relationships were obtained using a ramp pulse from −50 mV to +50 mV at peak current (B). (**D–F**) Single-channel recordings were performed in the cell-attached configuration with cAMP cocktail stimulation. Current records at −80 mV (D) were analyzed to estimate the open probability (Po) (F). Unitary conductance was calculated using all point histograms constructed for voltages ranging from −120 to +120 mV at 40 mV intervals. An example at +80 mV is shown in (E). (C) and (F) summarize the results from eight to 10 experiments for each mutant. $*P < 0.05$, $**P < 0.01$ difference from WT.

**Table 4.** Characteristics of CFTR mutants selected for functional studies

| Name | Nucleotide change | Exon | Domain | Evolutionary conservation[a] | Possible disease association[b] |
|---|---|---|---|---|---|
| E217G | 782A > G | 6a | EC2 | b, h, r | CF with pancreatic sufficiency (Polish), Panbronchiolitis (Japanese) |
| I556V | 1798A > G | 11 | NBD1 | All seven species | Chronic bronchitis (French) |
| Q1352H | 4188G > C | 22 | NBD2 | All seven species | CBAVD (Japanese), Panbronchiolitis (Japanese) |
| R1453W | 4489C > T | 24 | IC10 | b, h, m, r, s | Panbronchiolitis (Japanese) |

[a]Evolutionary conservations are compared in CFTR genes of bovine (b), dogfish (d), human (h), mouse (m), rabbit (r), sheep (s), and xenopus (x).
[b]Notes reported to CFGAC. CBAVD, congenital bilateral absence of vas deferens; CF, cystic fibrosis; EC, extracellular domain; IC, intracellular domain; NBD, nucleotide binding domain.

in a control subject. One of the interesting observations was the rare frequency of haplotype 12 in the Korean population (0.9%). This haplotype has IVS8 $T_9$-M470-2694T and it corresponds to haplotype IIIa of Cuppens' report (8). The frequency of this haplotype is 7.3% in the normal Belgian population. However, over 95% of the three most common CF-causing mutations, F508del, G542X and N1303K, arise from this haplotype. For some reason, the gene flow or selection pressure for this haplotype has been extremely low in the Korean population. Thus, we postulate that the low frequency of haplotype 12 is the principal reason for the rare incidence of classical CF in East Asia.

It is known that polymorphisms in IVS8 $T_n$ affect the RNA splicing of exon 9, and that the IVS8 $T_5$ variation reduces splice

Downloaded from https://academic.oup.com/hmg/article-abstract/12/18/2321/2355638 by guest on 13 October 2019

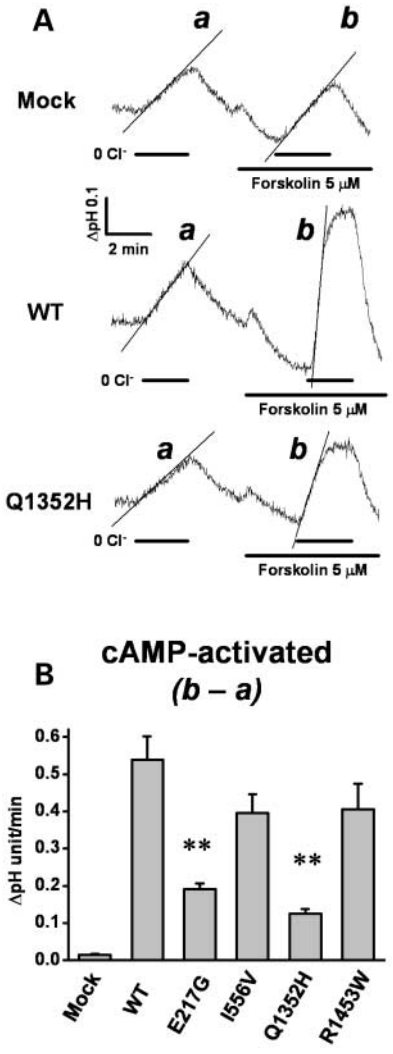


**Figure 4.** Measurements of CFTR-dependent $Cl^-/HCO_3^-$ exchange. Coverslip-grown CHO cells were loaded with BCECF and $pH_i$ was measured in a perifusion chamber. $Cl^-/HCO_3^-$ exchange activities were estimated from the initial rate of $pH_i$ increase after $Cl^-_0$ removal in the $HCO_3^-$ buffered perfusate (25 mM $HCO_3^-$ with 5% $CO_2$). After determining the basal activity, the forskolin-stimulated (5 μM) activities were measured. Representative traces of Mock-, WT- and Q1352H-transfected cells are shown in (**A**), and the results of five to six experiments for each mutant are summarized in (**B**). $^{**}P < 0.01$ difference from WT.

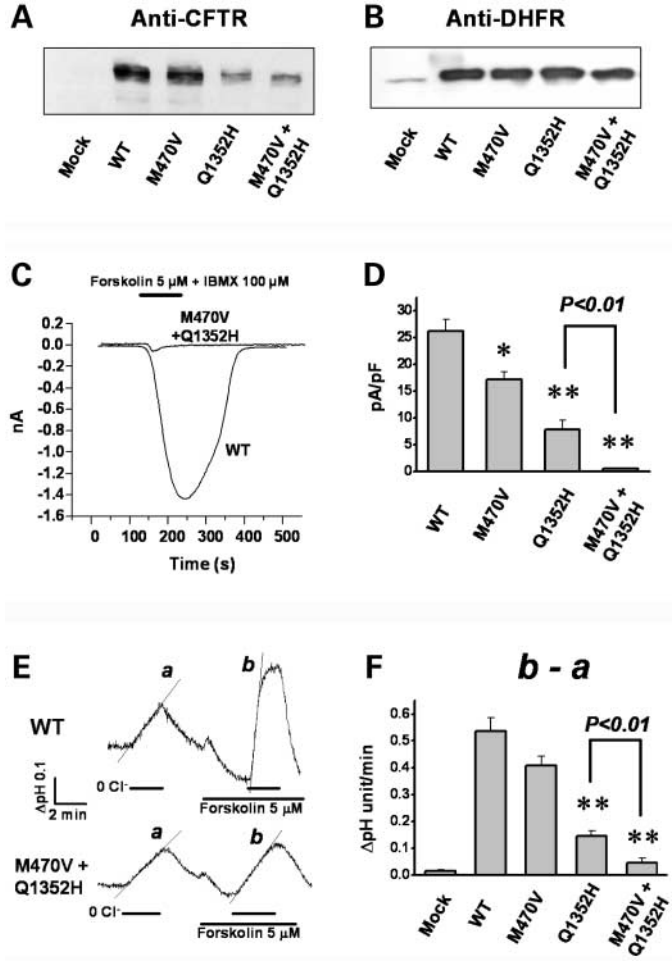


**Figure 5.** Effects of M470V on Q1352H mutant. M470V variation was introduced in the WT and the Q1352H clones and protein expressions and functional activities were measured using the protocols described in the legends of Figures 2–4. M470V change did not alter the protein expression levels in WT- or Q1352H-CFTR (**A**, **B**). However, additional M470V change in Q1352H abolished cAMP-activated $Cl^-$ currents (**C**, **D**) and $Cl^-/HCO_3^-$ exchanges (**E**, **F**). $^*P < 0.05$, $^{**}P < 0.01$ difference from WT.

acceptor efficiency. Hence, this variation reduces proper RNA and protein synthesis and seems to be associated with CF and/or CF-related diseases, such as congenital bilateral absence of vas deferens (CBAVD). In addition, it was suggested that when IVS8 $T_5$ is combined with additional activity-reducing variations, such as the higher number of IVS8 $(TG)_m$ and the V470 variant, it shows higher disease penetrance (16). Although $(TG)_m$ was not analyzed in this study, the results of the M470V polymorphism support this notion. Of the two IVS8 $T_5$ containing haplotypes (haplotypes 5 and 9), only haplotype 5, which also has the low activity variation of V470, showed an association with the disease phenotype (Table 3). Interestingly, a case of $T_6$ was found in a bronchiectasis patient in addition to the well-known $T_5$, $T_7$ and $T_9$ alleles. However, its disease association is uncertain at this moment, and future functional transcript studies are required to assess its clinical relevance.

Q1352H was found to be the most notable mutation in both case–control and molecular functional studies. It is located in a conserved glutamine-rich sequence, called the 'linker peptide', 'signature motif' or 'motif C' in the second nucleotide binding domain (NBD2) of CFTR. In a structural study of the NBD domain of a bacterial ABC transporter, it was suggested that the linker peptide would be an essential motif for the integrity of folded NBD structures and for the regulation of ATP hydrolysis (24). Our observations are wholly in accord with this suggestion. The linker region of CFTR NBD2 is composed of 'LSHGHKQ' and differs slightly from the classic linker sequence of 'LSGGQ'. However, its sequence is highly conserved in all vertebrates and the change of the last glutamine into histidine (Q1352H) evoked defects in protein

Downloaded from https://academic.oup.com/hmg/article-abstract/12/18/2321/2355638 by guest on 13 October 2019

expression and affected the gating properties of single channel kinetics (Figs 2 and 3).

E217G was previously identified in a Polish CF patient with pancreatic sufficiency (data from CFGAC) and showed a marginal disease association in the present case–control study. These results imply that E217G is a mild mutation, which is also supported by our molecular data. The E217G mutation partially decreased membrane protein expression and anion transporting activities by 60–70%. However, the strongly disease associated Q1352H mutation also decreased the protein expression and functional activities by only 70–80%, which was not much different from E217G when they were measured in the same haplotype background of M470 (Figs 2–4). Of interest, E217G was found to arise in the haplotype having a high activity type of M470 (haplotype 6), and Q1352H to arise in the low activity type of V470 (haplotype 4) in the real population. Therefore, combinatorial effects with M470V locus may influence the overall function of haploid gene products in Q1352H mutation. Indeed, molecular data of double mutagenesis showed a surprising result that the additional change of M470V in Q1352H abolished the anion transporting activities of CFTR protein (Fig. 5). The reasons for the complete reduction of functional activities are unclear at this moment. A plausible scenario is that M470V and Q1352H might be involved in the cross talk and/or interaction between the two NBDs of CFTR (25,26), since M470V and Q1352H are located in the NBD1 and NBD2, respectively. Although it was previously suggested that V470 may affect CFTR function (5,16), this is the first report directly showing that *cis*-interaction of V470 determines the disease status of a mutant CFTR gene. The above results suggest that multiple genetic variations in CFTR gene can affect the overall function of the protein and the intensity of the disease association. In this regard, haplotype-based approaches should be emphasized and encouraged to evaluate the disease associations not only of CFTR genes, but also of candidate genes in other diseases.

In the case–control analysis, overall statistical significances were analyzed by the Bonferroni technique and the summation of chi-square method. However, the two methods showed contradictory results. These phenomena are frequently confronted in the genetic association studies for multiple loci analysis (17), and it is still the subject of debate as to what kind of statistical test will be ideal to assess the clinical study with multiple measures (27,28). If the conservative Bonferroni technique is adopted, positive findings are hardly observed in most studies and the risk of false negative (type II error) is increased, especially for mutations with rare incidences. In contrast, if we simply accept $P < 0.05$ at single locus analysis, the risk of false positive (type I error) will be increased. Therefore, it was once suggested that the summation of chi-square statistics followed by an analysis of individual loci would be the most appropriate approach (17). However, others do not completely agree with this type of approach and suggest other statistical methods (27,28). In the present study, to minimize the possible errors, we employed the integrated approach that identifies the possible disease-associated variations from the population data using conventional statistics and then verifies the functions of their gene products at the molecular level. We believe this method is a very effective approach to assess the clinical relevance of gene variations and to overcome the statistical limitations.

In conclusion, CFTR mutations of M470V-Q1352H, IVS8 $T_5$-M470V, and E217G are associated with bronchiectasis and chronic pancreatitis. In the enrolled Korean population, ~20% of patients with bronchiectasis and chronic pancreatitis of an unknown etiology possessed CFTR haploid genes bearing the above mutations. Defects in CFTR-dependent ion transport are an important aggravating factor in the disease development and/or progression in addition to other genetic and environmental factors.

## MATERIALS AND METHODS

### Studied samples

This study was approved by the institutional review board of Yonsei Medical Center, Seoul, Korea. A series of 75 unrelated Korean patients having disseminated bronchiectasis or chronic pancreatitis of unknown origin were enrolled after giving informed consent. The bronchiectasis group was composed of 20 pediatric patients (ages 1–18) and 27 adult patients (ages 22–74), and the diagnosis of disseminated bronchiectasis was confirmed by high-resolution computer tomography. Among the adult bronchiectasis patients, 15 patients had a history of childhood onset and 10 patients had accompanying asthma symptoms. All the enrolled bronchiectasis patients did not have the symptoms and signs related to classical CF, such as predominant upper lobe involvement, malabsorption and intestinal obstruction. The 28 chronic pancreatitis patients were diagnosed based on standard criteria, which included abnormalities on histologic analysis of biopsy specimens, visible calculi on radiologic examinations, or unequivocally abnormal findings by endoscopic pancreaticography in addition to their compatible clinical presentations. Alcoholic subjects taking over 40 g of ethanol daily were excluded from the study. One-hundred and seventeen healthy control subjects were randomly selected, and their health statuses were evaluated by routine physical examinations, laboratory tests and radiologic examinations. Blood samples were collected from each subject and DNA was extracted using a purification kit (Qiagen).

### Genetic analysis

The mutation/polymorphism pattern of the CFTR gene in the Korean population was scanned using the two-dimensional gene scanning (TDGS) method. PCR primer sets for the human CFTR gene designed for TDGS analysis were purchased from Accelerated Genomics Inc. (San Antonio, TX, USA) and the individual primer sequences without GC clamps are listed in the Supplementary Material. To increase the efficiency of TDGS, primers were fluorescently labeled with HEX and GC-clamps were attached to one primer of each pair (29). The entire CFTR coding regions and flanking intronic sequences were amplified by a two-step multiplex PCR reaction. First, a 9-plex long distance PCR was performed to amplify nine large fragments encompassing the coding regions of CFTR. These products then served as templates for four multiplex short PCR reactions to amplify all 41 target fragments between 100 and 500 bp long.

Downloaded from https://academic.oup.com/hmg/article-abstract/12/18/2321/2355638 by guest on 13 October 2019

Subsequently, PCR fragments were subjected to one round of complete denaturation and renaturation to create heteroduplex molecules. The mixture of all CFTR fragments was loaded onto an automated two-dimensional gel electrophoresis instrument (OptiAnalyzer 8008HT; Accelerated Genomics), and separated simultaneously in a DGGE gel according to their fragment size and melting temperature. The entire DNA fragments were visualized by a fluorescent scanner (Molecular Imager FX, Bio-Rad) and heterozygous polymorphisms or mutations were detected as four spots rather than one spot, representing the two homoduplex and the two heteroduplex variants. The nature and location of sequence variations were identified by DNA nucleotide sequence analysis (Fig. 1).

Genotype characterization of the diallelic loci was performed by the SNaPshot method (Applied Biosystems, Foster City, CA, USA) according to the protocol supplied by the manufacturer on an automated genetic analyzer (Model 3700, Applied Biosystems) and polymorphisms in the IVS8 $T_n$ microsatellite were analyzed by bi-directional nucleotide sequencing.

Haplotype assembly was performed using the Haplotyper program based on the Bayesian algorithm to reconstruct individual haplotypes from population genotype data (7). Data on the 10 diallelic variations, which actually exist in the Korean population, and polymorphisms in IVS8 $T_n$ were used to generate haplotypes (Table 3). Output consisted of two parts, individual haplotype information and haplotype pool information.

### Site-directed mutagenesis and expression of CFTR

The use of pNUT-CFTR plasmid for the stable expression of human wild-type CFTR in mammalian cells has been described previously (30). The plasmid also contains the gene for dihydrofolate reductase (DHFR), which enables the selection of transfectants with methotrexate. Site-directed mutagenesis at four non-synonymous mutations (Table 4) and M470V was performed using the QuickChange mutagenesis kit from Stratagene (La Jolla, CA, USA). The plasmids for WT and mutant CFTR expression were transfected into a DHFR-negative CHO-K1 cell line (KCLB 10061; Korea Cell Line Bank, Seoul, Korea) using LipofectAMINE Plus reagent (Life Technologies). CHO-K1 cells were maintained in RPMI1640 medium supplemented with 10% fetal calf serum and penicillin (50 units/ml)/streptomycin (50 μg/ml). Two days after transfection, methotrexate (500 μg/ml, Alexis) was added to the culture medium for the selection of transfected cells. For each mutant, two or three separate stable cell lines were developed using different batches of clones to confirm similar mutation-induced functional changes. The mutagenic primers were as follows: E217G, 5′-CTC CTC ATG GGG CTA ATC TGG **GGG** TTG TTA CAG GCG TCT G-3′ M470V, 5′-CTG GAG CAG GCA AGA CTT CAC TTC TAA TG**G TG**A TTA TGG GAG-3′; I556V, 5′-AGT GGA GGT CAA CGA GCA AGA **GTT** TCT TTA GCA AGG TGA AT-3′; Q1352H, 5′-CCT AAG CCA TGG CCA CAA G**CA CT**T GAT GTG CTT GGC TAG-3′; R1453W, 5′-GTG AAG CTC TTT CCC CAC **TGG** AAC TCA AGC AAG TGC AAG TCT-3′.

### Immunoblotting of CFTR and DHFR

CHO-K1 cells transfected with pNUT-CFTR vector were trypsinized, and lysed with a standard lysis buffer containing protease inhibitor cocktails. Fifty micrograms of protein samples from WT or mutant CFTR-expressing cells were suspended in SDS sample buffer and separated by SDS–PAGE on 6% gels. The separated proteins were transferred to a nitrocellulose membrane and probed with the monoclonal antibody M3A7 against the NBD2 domain of CFTR (Upstate Biotech). After treating with appropriate secondary antibody, protein bands were visualized using an enhanced chemiluminescence kit (Amersham Pharmacia). To normalize the transfection levels of the pNUT-CFTR plasmids, the expression levels of a *cis*-gene product DHFR were analyzed by immunoblotting with smaller amount of lysate (10 μg protein) and anti-DHFR antibodies (Research Diagnostics Inc.). Staining intensities of CFTR and DHFR bands were analyzed using an imaging software (MCID version 3.0; Brook University, St Catharines, Ontario, Canada) and the intensity ratios of CFTR/DHFR were compared in each mutant transfected cells.

### Measurement of $Cl^-$ channel activities

Initially, whole-cell recordings were performed on transfected CHO-K1 cells. The pipette solution contained (in mM) 140 *N*-methyl D-glucamine chloride (NMDG-Cl), 5 EGTA, 1 $MgCl_2$, 1 Tris–ATP and 10 HEPES (pH 7.2), and the bath solution contained (in mM) 140 NMDG-Cl, 1 $CaCl_2$, 1 $MgCl_2$, 10 glucose and 10 HEPES (pH 7.4). All experiments were performed at room temperature (22–25°C). Pipettes were pulled from borosilicate glass and had resistances of 3–5 MΩ after fire polishing. Seal resistances were typically between 3 and 10 GΩ. After establishing the whole-cell configuration, CFTR was activated by adding 5 μM forskolin and 100 μM 3-isobutyl-1-methylxanthine (IBMX). The holding potential used in the capacitance experiments was −30 mV and the patch-clamp output was filtered at 5 kHz. Currents were digitized and analyzed using an AxoScope 8.1 system and a Digidata 1322A AC/DC converter. Mean currents were normalized as current densities (pA/pF).

Single channel characteristics of WT and mutant CFTR were analyzed in the cell-attached configuration using fire-polished pipettes with a resistance of 10–17 MΩ. The pipette solution contained (in mM) 140 NMDG-Cl, 1.3 $CaCl_2$, 1 $MgCl_2$, 5 glucose and 10 HEPES (pH 7.4), and the KCl bath solution contained 140 KCl, 1.3 $CaCl_2$, 1 $MgCl_2$, 5 glucose and 10 HEPES (pH 7.4). Recordings were performed at room temperature using an Axopatch-200B (Axon Instruments). The voltage and current data were low-pass filtered at 1 kHz and stored for later analysis. Single channel data were digitally filtered at 25 Hz, and analyzed using Fetchan and pSTAT v6.0 softwares (Axon Instruments).

### Measurement of $Cl^-/HCO_3^-$ exchange

$Cl^-/HCO_3^-$ exchange activity was measured by recording the intracellular pH ($pH_i$) in response to $[Cl^-]_o$ changes of the

Downloaded from https://academic.oup.com/hmg/article-abstract/12/18/2321/2355638 by guest on 13 October 2019

perfusate, as previously detailed (11). In brief, cell-attached glass coverslips were washed once with HEPES-buffered solution A and assembled to form the bottom of a perfusion chamber. The HEPES-buffered solution A contained (in mM) 140 NaCl, 5 KCl, 1 $MgCl_2$, 1 $CaCl_2$, 10 glucose and 10 HEPES (pH 7.4). Cells were loaded with a fluorescent pH probe BCECF by incubating for 10 min at room temperature in solution A containing 2.5 μM BCECF-AM. After dye loading, the cells were perfused with a $HCO_3^-$-buffered solution and BCECF fluorescence was recorded at the excitation wavelengths of 490 and 440 nm at a resolution of 2/s using a recording setup (Delta Ram; PTI Inc.). The $HCO_3^-$-buffered solution contained (in mM) 120 NaCl, 5 KCl, 1 $MgCl_2$, 1 $CaCl_2$, 10 glucose, 5 HEPES, 25 $NaHCO_3$ (pH 7.4) and was continuously gassed with 95% $O_2$ and 5% $CO_2$. $Cl^-$-free solutions were prepared by replacing the $Cl^-$ with gluconate. The 490/440 ratios were calibrated intracellularly by perfusing the cells with solutions containing 145 mM KCl, 10 mM HEPES, and 5 μM nigericin with the pH adjusted to 6.2–7.6.

### Statistical analysis

To analyze genotype and haplotype data (Tables 2 and 3), differences between control and disease groups were compared by a chi-square test. When an expected cell value was less than 5, Fisher's exact test was used. Two different methods, the Bonferroni technique and the summation of chi-square statistics, were used to evaluate the overall statistical significance of multiple comparisons (17). In the case of functional measurements of $Cl^-$ currents and of $Cl^-/HCO_3^-$ exchange (Figs 2–4), analysis of variance was used. All *P*-values were based on two-sided comparisons and *P*-values of less than 0.05 were considered to indicate statistical significance.

## SUPPLEMENTARY MATERIAL

Supplementary Material is available at HMG Online.

## ACKNOWLEDGEMENTS

We thank Dr Jan Vijg (University of Texas Health Science Center at San Antonio) for technical advice on CFTR-TDGS, and Dr Shmuel Muallem (University of Texas Southwestern Medical Center at Dallas) for helpful discussions. We also thank WonSun Han for her editorial assistance. This work was supported by grant R01-2001-000-00208-0 from the Korea Science and Engineering Foundation (K.H.K.) and grant 02-PJ1-PG3-21499-0003 from the Ministry of Health and Welfare, Korea (M.G.L.).

## REFERENCES

1. Riordan, J.R., Rommens, J.M., Kerem, B., Alon, N., Rozmahel, R., Grzelczak, Z., Zielenski, J., Lok, S., Plavsic, N., Chou, J.L. *et al.* (1989) Identification of the cystic fibrosis gene: cloning and characterization of complementary DNA. *Science*, **245**, 1066–1073.
2. Pignatti, P.F., Bombieri, C., Marigo, C., Benetazzo, M. and Luisetti, M. (1995) Increased incidence of cystic fibrosis gene mutations in adults with disseminated bronchiectasis. *Hum. Mol. Genet.*, **4**, 635–639.
3. Sharer, N., Schwarz, M., Malone, G., Howarth, A., Painter, J., Super, M. and Braganza, J. (1998) Mutations of the cystic fibrosis gene in patients with chronic pancreatitis. *New Engl. J. Med.*, **339**, 645–652.
4. Cohn, J.A., Friedman, K.J., Noone, P.G., Knowles, M.R., Silverman, L.M. and Jowell, P.S. (1998) Relation between mutations of the cystic fibrosis gene and idiopathic pancreatitis. *New Engl. J. Med.*, **339**, 653–658.
5. Wang, X., Moylan, B., Leopold, D.A., Kim, J., Rubenstein, R.C., Togias, A., Proud, D., Zeitlin, P.L. and Cutting, G.R. (2000) Mutation in the gene responsible for cystic fibrosis and predisposition to chronic rhinosinusitis in the general population. *JAMA*, **284**, 1814–1819.
6. Groman, J.D., Meyer, M.E., Wilmott, R.W., Zeitlin, P.L. and Cutting, G.R. (2002) Variant cystic fibrosis phenotypes in the absence of CFTR mutations. *New Engl. J. Med.*, **347**, 401–407.
7. Niu, T., Qin, Z.S., Xu, X. and Liu, J.S. (2002) Bayesian haplotype inference for multiple linked single-nucleotide polymorphisms. *Am. J. Hum. Genet.*, **70**, 157–169.
8. Cuppens, H., Teng, H., Raeymaekers, P., De Boeck, C. and Cassiman, J.J. (1994) CFTR haplotype backgrounds on normal and mutant CFTR genes. *Hum. Mol. Genet.*, **3**, 607–614.
9. Morral, N., Bertranpetit, J., Estivill, X., Nunes, V., Casals, T., Gimenez, J., Reis, A., Varon-Mateeva, R., Macek, M. Jr, Kalaydjieva, L. *et al.* (1994) The origin of the major cystic fibrosis mutation (ΔF508) in European populations. *Nat. Genet.*, **7**, 169–175.
10. Schwiebert, E.M., Benos, D.J., Egan, M.E., Stutts, M.J. and Guggino, W.B. (1999) CFTR is a conductance regulator as well as a chloride channel. *Physiol Rev.*, **79** (Suppl. 1), S145–S166.
11. Lee, M.G., Wigley, W.C., Zeng, W., Noel, L.E., Marino, C.R., Thomas, P.J. and Muallem, S. (1999) Regulation of $Cl^-/HCO_3^-$ exchange by cystic fibrosis transmembrane conductance regulator expressed in NIH 3T3 and HEK 293 cells. *J. Biol. Chem.*, **274**, 3414–3421.
12. Lee, M.G., Choi, J.Y., Luo, X., Strickland, E., Thomas, P.J. and Muallem, S. (1999) Cystic fibrosis transmembrane conductance regulator regulates luminal $Cl^-/HCO_3^-$ exchange in mouse submandibular and pancreatic ducts. *J. Biol. Chem.*, **274**, 14670–14677.
13. Ahn, W., Kim, K.H., Lee, J.A., Kim, J.Y., Choi, J.Y., Moe, O.W., Milgram, S.L., Muallem, S. and Lee, M.G. (2001) Regulatory interaction between the cystic fibrosis transmembrane conductance regulator and $HCO_3^-$ salvage mechanisms in model systems and the mouse pancreatic duct. *J. Biol. Chem.*, **276**, 17236–17243.
14. Namkung, W., Lee, J.A., Ahn, W., Han, W., Kwon, S.W., Ahn, D.S., Kim, K.H. and Lee, M.G. (2003) $Ca^{2+}$ activates cystic fibrosis transmembrane conductance regulator- and $Cl^-$-dependent $HCO_3^-$ transport in pancreatic duct cells. *J. Biol. Chem.*, **278**, 200–207.
15. Wu, Y., Hofstra, R.M., Scheffer, H., Uitterlinden, A.G., Mullaart, E., Buys, C.H. and Vijg, J. (1996) Comprehensive and accurate mutation scanning of the CFTR gene by two-dimensional DNA electrophoresis. *Hum. Mutat.*, **8**, 160–167.
16. Cuppens, H., Lin, W., Jaspers, M., Costes, B., Teng, H., Vankeerberghen, A., Jorissen, M., Droogmans, G., Reynaert, I., Goossens, M., Nilius, B. and Cassiman, J.J. (1998) Polyvariant mutant cystic fibrosis transmembrane conductance regulator genes. The polymorphic $(TG)_m$ locus explains the partial penetrance of the $T_5$ polymorphism as a disease mutation. *J. Clin. Invest.*, **101**, 487–496.
17. Ryman, N. and Jorde, P.E. (2001) Statistical power when testing for genetic differentiation. *Mol. Ecol.*, **10**, 2361–2373.
18. Ward, C.L., Omura, S. and Kopito, R.R. (1995) Degradation of CFTR by the ubiquitin-proteasome pathway. *Cell*, **83**, 121–127.
19. Wigley, W.C., Fabunmi, R.P., Lee, M.G., Marino, C.R., Muallem, S., DeMartino, G.N. and Thomas, P.J. (1999) Dynamic association of proteasomal machinery with the centrosome. *J. Cell Biol.*, **145**, 481–490.
20. Anderson, M.P., Rich, D.P., Gregory, R.J., Smith, A.E. and Welsh, M.J. (1991) Generation of cAMP-activated chloride currents by expression of CFTR. *Science*, **251**, 679–682.
21. Kartner, N., Hanrahan, J.W., Jensen, T.J., Naismith, A.L., Sun, S.Z., Ackerley, C.A., Reyes, E.F., Tsui, L.C., Rommens, J.M. and Bear, C.E. (1991) Expression of the cystic fibrosis gene in non-epithelial invertebrate cells produces a regulated anion conductance. *Cell*, **64**, 681–691.

Downloaded from https://academic.oup.com/hmg/article-abstract/12/18/2321/2355638 by guest on 13 October 2019

22. Choi, J.Y., Muallem, D., Kiselyov, K., Lee, M.G., Thomas, P.J. and Muallem, S. (2001) Aberrant CFTR-dependent $HCO_3^-$ transport in mutations associated with cystic fibrosis. *Nature*, **410**, 94–97.
23. Quinton, P.M. (2001) The neglected ion: $HCO_3^-$. *Nat. Med.*, **7**, 292–293.
24. Hung, L.W., Wang, I.X., Nikaido, K., Liu, P.Q., Ames, G.F. and Kim S.H. (1998) Crystal structure of the ATP-binding subunit of an ABC transporter. *Nature*, **396**, 703–707.
25. Carson, M.R, Travis, S.M. and Welsh, M.J. (1995) The two nucleotide-binding domains of cystic fibrosis transmembrane conductance regulator (CFTR) have distinct functions in controlling channel activity. *J. Biol. Chem.*, **270**, 1711–1717.
26. Wei, L., Vankeerberghen, A., Jaspers, M., Cassiman, J., Nilius, B. and Cuppens, H. (2000) Suppressive interactions between mutations located in the two nucleotide binding domains of CFTR. *FEBS Lett.*, **473**, 149–153.
27. Perneger, T.V. (1988) What's wrong with Bonferroni adjustments. *Br. Med. J.*, **316**, 1236–1238.
28. Sterne, J.A.C. and Smith, G.D. (2001) Sifting the evidence-what's wrong with significance tests? *Br. Med. J.*, **322**, 226–231.
29. McGrath, S.B., Bounpheng, M., Torres, L., Calavetta, M., Scott, C.B., Suh, Y., Rines, D., van Orsouw, N. and Vijg, J. (2001) High-speed, multicolor fluorescent two-dimensional gene scanning. *Genomics*, **78**, 83–90.
30. Tabcharani, J.A., Chang, X.-B., Riordan, J.R. and Hanrahan. J.W. (1991) Phosphorylation-regulated $Cl^-$ channel in CHO cells stably expressing the cystic fibrosis gene. *Nature*, **352**, 628–631.

Downloaded from https://academic.oup.com/hmg/article-abstract/12/18/2321/2355638 by guest on 13 October 2019